Numerical Investigation Of Airflow In An Open Geometry

Boris Brangeon, Alain Bastide, Patrice Joubert

NUMERICAL INVESTIGATION OF AIRFLOW IN AN OPEN GEOMETRY

Boris Brangeon[1], Alain Bastide[1], Patrice Joubert[2], Michel Pons[3]
[1]PIMENT, Université de La Réunion, 117 Avenue du Général Ailleret 97430 Le Tampon, France.
[2]LEPTIAB, Université de La Rochelle, Avenue M. Crépeau, 17042 La Rochelle Cedex 1, France.
[3]LIMSI CNRS UPR3251, BP 133, 91403 Orsay Cedex, France.

Abstract

This paper presents a numerical investigation of airflow in an open geometry. The case under consideration is room with two opposite and decentred openings which create a strong potential for ventilation. The building characteristics dimensions are the followings: H=2.50 m height and W=6.50 m width. A temperature difference between the walls and the outside air is fixed, resulting in a characteristic Rayleigh number (Ra) ranging from 10^5 to 1.49 10^8. This room model proceeds from a benchmark exercise "ADNBATI" (http://adnbati.limsi.fr) coordinated by the by the "Centre National de la Recherche Française -CNRS-". This paper presents and discusses the results of this numerical study. Velocity, temperature fields, as well as heat transfer at the walls are analyzed. Values of the Nusselt number and of the mass flow rate according to the Rayleigh number are established from these first results.

Keywords: Direct Numerical Simulation, Natural convection, Open enclosures, Boundary conditions.

1 Introduction

For night cooling of buildings, two choices are possible: mechanical ventilation and/or natural ventilation. This later mechanism is an efficient passive cooling process for moderate hot climates and is investigated in this paper to remove excessive heat accumulated during the day. The geometrical configuration is an open room with two opposite and decentred openings to create a strong potential for natural ventilation. The room model proceeds from a benchmark exercise "ADNBATI" (Stephan, 2010) coordinated by the "Centre National de la Recherche Française -CNRS-". The building characteristics dimensions are the followings: H=2.50 m height and W=6.50 m width (Fig.1). The opening ratio H_1/H_2 equals 0.5. Ra is the Rayleigh number based on the cavity height H. A temperature difference between the inside walls and the outside air is fixed, resulting in a characteristic Rayleigh number ranging from 10^5 to 1.49 10^8.

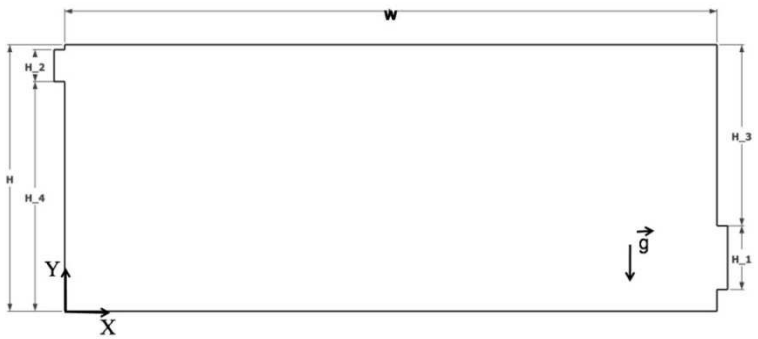

***Figure 1**. Cavity problem.*

***Table 1**. Geometry characteristics parameters.*

	Value [m]
Height low East opening H_1	0.6
Height low West opening H_2	0.3
Height wall East H_3	1.7
Height wall West H_4	2.15

2 Methods

2.1 Governing equations

We consider a cavity of height H and width W traversed with an incompressible Newtonian viscous fluid of kinematic viscosity ν and thermal diffusivity κ (Fig. 1). The fluid density ρ is assumed to depend only on temperature : $\rho = \rho_0[1 - \beta(T - T_0)]$, where β is the thermal expansion coefficient. Due to the thermal boundary conditions radiative transfer are neglected. The usual dimensionless Boussinesq 2D Navier-Stokes equations are then:

$$\frac{\partial u}{\partial x} + \frac{\partial v}{\partial y} = 0 \tag{1}$$

$$\frac{\partial u}{\partial t} + u\frac{\partial u}{\partial x} + v\frac{\partial u}{\partial y} = -\frac{\partial P_m}{\partial x} + PrRa^{-1/2}\nabla^2 u \tag{2}$$

$$\frac{\partial v}{\partial t} + u\frac{\partial v}{\partial x} + v\frac{\partial v}{\partial y} = -\frac{\partial P_m}{\partial y} + PrRa^{-1/2}\nabla^2 v + Pr\theta \tag{3}$$

$$\frac{\partial \theta}{\partial t} + u\frac{\partial \theta}{\partial x} + v\frac{\partial \theta}{\partial y} = Ra^{-1/2}\nabla^2 \theta \tag{4}$$

The corresponding equations are made dimensionless by introducing H, $U_{CN} = \kappa Ra^{1/2}/H$ (Bejan, 1984) and ΔT as refernce quantities for length, velocity and temperature difference. The Prandtl number Pr is fixed to 0.71.

2.2 Boundary conditions

The walls temperature are set to a constant temperature, Tw, higher than the outside temperature except for the frames of the openings for which an adiabatic condition is applied (Fig. 1). A non-slip boundary condition is imposed on the velocity along all the walls.

Low East opening/ high West opening: the openings are framed, in order to take the thickness of the walls into account. The imposed conditions at the end of these frames (X = −0.1 m and X = 6.6 m) are the followings: if V.n<0 then θ=0, else $\frac{\partial \theta}{\partial x} = 0$.

The choice of the boundary conditions that must be applied to the velocity and the pressure is delicate for open geometries with natural convection flow. Indeed, the resulting thermosiphon flow is the result of the balance between the forces due to buoyancy and the head losses between the low East and the high West openings of the cavity. However, no choice appears to be trivial to impose velocity or pressure conditions at the low East opening. We use here an original boundary condition to the openings. We admit that at the low East opening, the following hypotheses are respected: the flow is steady and incompressible, the viscous terms are negligible and the rotational of the velocity equals zero. We can therefore relate the mass flow rate to the difference of pressure between the low East and the high West opening by the relation:

$$\int_{H_2} (p + \rho g z) \, . \, dA - \int_{H_1} (p + \rho g z) \, . \, dA = \int_{H_1} \frac{1}{2} \rho |v|^2 \, . \, dA \tag{5}$$

This boundary condition is identical to the one which was proposed during a set benchmark in the framework of the network AMETh (Desrayaud, 2007) constituted of an asymmetrically-heated vertical channel, treated experimentally by (Webb and Hill, 1989). The comparison of the two numerical simulations between different French research teams and our personal works, turns out to be conclusive for *Ra* equals to 5.10^5. The benchmark ADNBATI (Stephan, 2010) also questions this issue and is currently subjected to a confrontation between French teams using numerical research codes or commercial codes. In our simulation, the boundary conditions are:

- at the low East opening: if V.n<0 then $P_m = -\frac{1}{2{S_e}^2} G^2$ where n is exterior normal vector, *G* is mass flow rate and S_e is low East opening section. Locally, if V.n>0 then $P_m = -\frac{1}{2}|v|^2$, else $P_m = 0$.
- at the high West opening: a free-jet condition is imposed: $P_m = 0$.

2.3 Numerical approach: spatial and temporal discretization

The numerical code has been developed thanks to the environment OpenFOAM (OpenFOAM, 2010). The time derivatives in the momentum and in the energy equations are performed by a second-order backward differentiation. The convections terms are approximated using a second-order Adams-Bashford extrapolation method. The diffusion terms are implicitly treated. The resulting Helmholtz systems are solved by a direct solver. Finally, the general numerical scheme is the following:

$$\frac{3f^{n+1} - 4f^n + f^{n-1}}{2\Delta t} + 2\left(\frac{\partial f u_j}{\partial x_j}\right)^n + \left(\frac{\partial f u_j}{\partial x_j}\right)^{n-1} = \left(\frac{\partial}{\partial x_j}\frac{\partial f}{\partial x_j}\right)^{n+1} \tag{6}$$

Pressure-velocity coupling is obtained by an incremental rotational projection method.

In the present study, a collocated finite volume method has been used. The case has been computed with a 1024×825 grid size. The local Reynolds number (*Re*) obtained is lower than 20 and the non-dimensional wall distance in terms of wall units (y^+) is less than 1. These quantities are regarded here for information on the quality of the mesh and will be submitted to an accurate study for more severe flows conditions for which turbulence models will be used. The dimensionless time step (Δt) varies from $1.25.10^{-4}$ (*Ra* = 10^5) to $0.85.10^{-4}$ (*Ra* = $1.49\ 10^8$).

3 Resultats and discusions

For this problem, the steady laminar flow observed at *Ra*=10^5 becomes unsteady at *Ra*=10^6, *Ra*=10^7 and *Ra*=$1.49\ 10^8$. In these later cases, once the established flow regime is observed, statistics are performed over a period of 60 non dimensional time units in order the statistical values associated with (u, v and θ).

Figure 2 displays the isotherms and streamlines fields for three values of the Rayleigh numbers: *Ra*= 10^5, 10^6 , 10^7 and $1.49\ 10^8$. In the four cases, the flow which goes from the low East opening to the high West opening splits into two parts. The main one is a cold jet, crawling along up to the West wall along which he finally goes up. The second moderate flow, turns right up along the East wall and joins the high West opening staying stuck to the ceiling. Between these two flows, two contrarotative cells exist, which progressively lengthen horizontally with increasing *Ra* values. The first of these cell is localized above the jet, in the main part of the cavity ($c_{1,10}^5$(x = 1.11; y = 0.47), $c_{1,10}^6$(x = 0.70; y =

0. 36), $c_{1,10}^{7}$(x = 0.52; y = 0.40), $c_{1,1.49\ 10}^{8}$(x = 0.57; y = 0.50)). The second one is located between the first cell and the heated surface of the ceiling ($c_{2,10}^{5}$ (x = 0.46; y =0.70), $c_{2,10}^{6}$ (x = 0.71; y = 0.70), $c_{1,1.49\ 10}^{8}$(x = 1.40; y = 0.58)). and becomes more and more intense for the successive values of *Ra*. The third large cell located along the East wall at $Ra=10^5$ moves progressively to the upper region of the vertical boundary layer and forms an hydraulic jump at the corner of the cavity, where the boundary layer experiences a sudden change in direction.

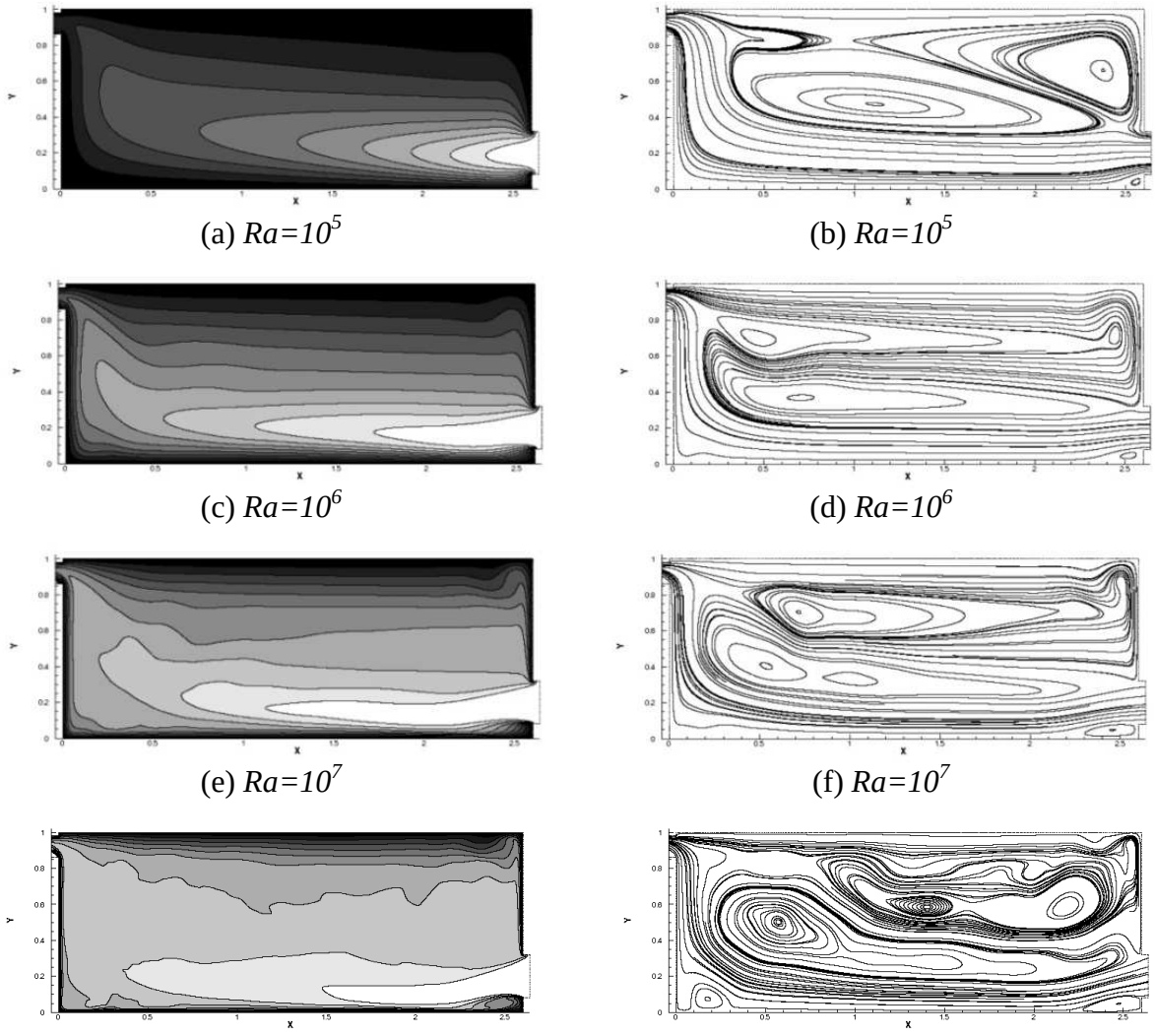

(a) $Ra=10^5$ (b) $Ra=10^5$

(c) $Ra=10^6$ (d) $Ra=10^6$

(e) $Ra=10^7$ (f) $Ra=10^7$

(g) $Ra=1.49\ 10^8$ (h) $Ra=1.49\ 10^8$

Figure 2. *Averaged solutions. Left: averaged temperature field. Right: streamlines of averaged flow.*

Additionally, a fresh air penetration becomes apparent and turns out to be stronger and stronger within the room with the increase of the Rayleigh number, that is to say when the convection acquires more and more importance compared to diffusion. The thickness of the boundary thermal layers decreases and the heart of the cavity cools down.

The third figure shows the evolution of the horizontal and vertical components of the velocity vector (respectively *U* and *V*) at the East opening (Fig. 3(a) and 3(b)) and to the West opening (Fig. 3(c) and 3(d)). The general velocity profiles at the East opening tends to distort it self and to crush when the temperature difference between the incoming air and the walls increases (Fig. 3(a)). This may be explained by a vertical, Rayleigh-Benard type instabilities that take place above the heated floor which to contradict the inlet jet. At the West opening, the fluid re-enters the cavity within a

height which can reach a quarter of the outlet section for $Ra = 10^6$-$1.49\ 10^8$. This phenomenon does not exist for the lower Rayleigh number.

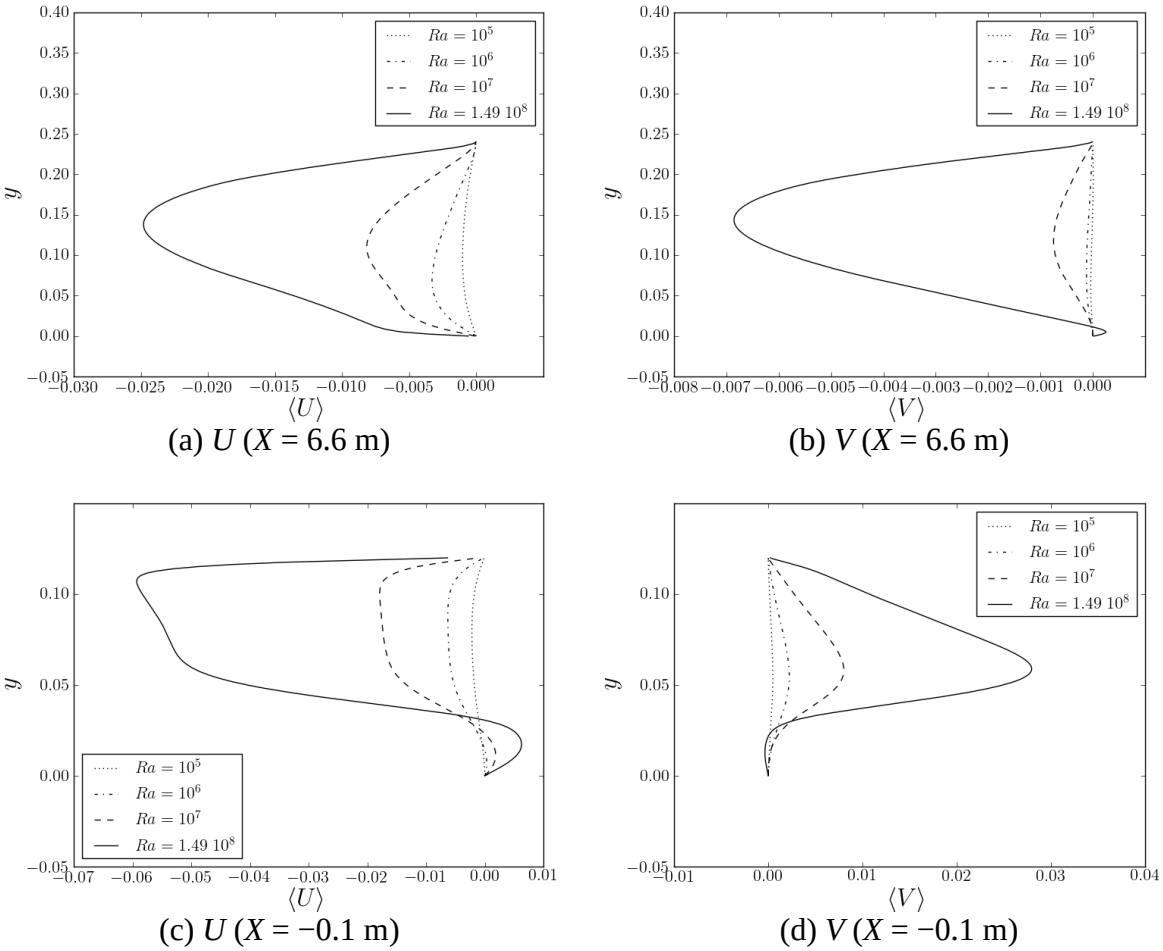

(a) U (X = 6.6 m) (b) V (X = 6.6 m)

(c) U (X = −0.1 m) (d) V (X = −0.1 m)

Figure 3*. Averaged horizontal (left) and vertical (right) velocity profiles at inlet: 3(a) et 3(b) and outlet: 3(c) et 3(d).*

The average values of the Nusselt number *Nu*, obtained along the hot vertical and horizontal walls are reported in table 2(a) (Nu_F stands the floor, Nu_R for the ceiling, Nu_O for the Western wall and Nu_E for the Eastern wall). The results indicate that the heat transfers are lower along the ceiling. For Ra=10^5, the convective exchange on the vertical Western wall is much more low than the one on the Eastern wall, even though these exchanges are balanced when *Ra* increases. This may be explained by the fact that for $Ra = 10^5$, the horizontal jet is weak and cannot drag the cold fluid up to the West wall. The mass flow rate in the cavity is presented in non dimensional (G) and dimensional (D_v) forms. The air regeneration rate (τ) is evaluated, as well as the average temperature of the exiting fluid at the high opening (θ_m). We observe that θ_m decreases when *Ra* increases, while D_v increases. It will be interesting in a next step to study if efficient air regeneration rate for night cooling process (typically τ of order 4-5) can be obtained by natural ventilation for Rayleigh numbers representative of real conditions, that is for Ra=10^{10}-10^{11}. This will be done with the help of a Large Eddy Simulation approach for turbulent flows.

Table 2. *Averaged Nusselt number (a) and summary of averaged flow results (b).*

Ra	10^5	10^6	10^7	$1.49\ 10^8$
Nu_F	3.60	8.01	17.95	41.27
Nu_R	0.80	1.49	2.97	7.44
Nu_O	1.58	7.21	17.41	43.38
Nu_E	3.41	7.49	17.60	40.11

(a)

Ra	10^5	10^6	10^7	$1.49\ 10^8$
G	0.023	0.021	0.018	0.014
D_v	0.223	0.654	1.775	5.58
τ	0.013	0.040	0.109	0.343
θ_m	0.850	0.700	0.550	0.405

(b)

4 Conclusion

A direct numerical simulation of the natural airflow in an open cavity has been presented and discussed. The room model we chose serves as a basis for other simulations in order to enrich our knowledge as regards to night cooling (benchmark configuration ADNBATI (Stephan, 2010). The first results obtained for *Ra* values ranging from 10^5 to $1.49\ 10^8$ will be confronted in a near future to other team's results. The future perspectives of this work would be, as an example, to establish a relationship between the Nusselt and the Rayleigh numbers ($Nu = \alpha Ra^{\gamma}$.) In order to reach/manage subsequently representative conditions of real conditions, $Ra = 10^{10}$-10^{11} it would be necessary to consider turbulence models in order to obtain computational time compatible with parametrical studies. In this idea, a Large Eddy Simulation approach will be implemented.

5 Acknowledgement

This work has been supported by French Research National Agency (ANR) through "Habitat intelligent et solaire photovoltaïque" program (project 4C n°ANR-08-HABISOL-019) and project "ADNBATI", financed by the Energy program of CNRS (PE09-3-2-1-1).

6 References

Bejan A. *Convection heat transfer*. John Wiley and Sons, 1984.

Desrayaud G., Bennacer R., Caltagirone J.P., Chenier E., Joulin A., Laaroussi N. and K.Mojtabi, *Etude numérique comparative des écoulements thermoconvectifs dans un canal vertical chauffé asymétriquement*. In VIIIème Colloque Interuniv. Franco-Québécois, Mai 2007, 6 pages.

Stephan L., Wurtz E., Bastide A., Brangeon B., Jay A., Goffaux C. and Pons C., *Benchmark de ventilation naturelle traversante* (ADNBATI). Actes Int. Building Performance Simulation Association (IBPSA-France) Conf., 9-10 Novembre 2010, Moret-sur-Loing, France, Ed. J. J. Roux & G. Krauss, Article 'PONS r98.doc', 2010.

Webb B.W and Hill D.P., *High Rayleigh number laminar natural convection in an asymmetrically heated vertical channel*. Journal Heat Transfer, (111), 1989, 649–656.

OpenFOAM 1.7, http ://www.openfoam.com, 2010.

Nomenclature

$c_{cell,Ra}$	convective cell center	[-]	U_{CN}	reference velocity	[-]
D_v	mass flow rate	[$m^2.h^{-1}$]	x, y	dimensionless spatial coordinate	[-]
G	dimensionless mass flow rate	[-]	X, Y	spatial coordinate	[m]
g	gravitational acceleration	[$m.s^{-2}$]	Pr	Prandtl number	[-]
H	cavity height	[m]			
H_1,H_2	height inlet and outlet	[m]			
H_3,H_4	height wall East and West	[m]	Greek symbols		
P_m	dimensionless dynamic pressure	[-]	β	thermal expansion	[K^{-1}]
Ra	Rayleigh number	[-]	κ	thermal diffusivity	[$m^2.s^{-1}$]
t	dimensionless time	[-]	ν	kinematic viscosity	[$m^2.s^{-1}$]
T	temperature	[K]	ρ	fluid density	[$kg.m^{-3}$]
ΔT	temperature difference	[K]	θ	dimensionless temperature	[-]
u, v	dimensionless velocity components	[-]	θ_m	dimensionless averaged temperature	[-]
U, V	velocity components	[$m.s^{-1}$]			